



# Reduction of fluid forces and vortex shedding frequency of a circular cylinder using rigid splitter plates

Rezvan Abdi<sup>a</sup> , Niki Rezazadeh<sup>a</sup> and Meisam Abdi<sup>b</sup>  

<sup>a</sup>Faculty of Engineering, Hakim Sabzevari University, Sabzevar, Iran; <sup>b</sup>Faculty of Engineering, University of Nottingham, Nottingham, UK

## ABSTRACT

This study investigates the fluid forces acting on a circular cylinder in a laminar flow regime while using a passive control strategy. Three cases including the cylinder with one, two or three rigid splitter plates attached at its rear surface were considered and the location of horizontal plates (attachment angle) was varied between 0° and 90°. A comprehensive parametric study was performed to identify the optimum arrangement of the plates using the commercial finite element software, Comsol Multiphysics. The results show that the location and the number of the plates have crucial effects on the wake control. Increasing the number of splitter plates from one to two symmetric parallel plates led to a reduction in drag force, vortex shedding frequency and fluctuation of lift force. A maximum drag reduction of 23% for dual-splitters and 15% for single-splitter was achieved, at an angle of 45° at Reynolds number 100. However, increasing the number of attached plates to three didn't have a significant effect on flow quantities when plates of the same length were utilised. The suitability of the third plate (the middle plate) was further studied by investigating the effect of length of the plate on flow quantities.

## ARTICLE HISTORY

Received 21 June 2016  
Accepted 12 March 2017

## KEYWORDS

Rigid splitter plate; vortex shedding; drag reduction; laminar flow; circular cylinder; Strouhal number

## 1. Introduction

As flow passes over a bluff body, two recirculating zones, known as vortices, are formed downstream of the bluff body. When Reynolds number ( $Re$ ) of the flow exceeds a threshold number, the vortices start to peel off periodically from the cylinder. When the vortex shedding occurs behind a cylinder, drag on the cylinder increases. Moreover, the periodic forces that were applied on the cylinder in the cross flow direction cause undesirable vibrations in the cylinder (Kwon & Choi, 1996). Many practical applications involve vortex-induced vibrations, including heat exchanger tube bundles, marine structures, bridges, power transmission lines

etc. Therefore, controlling the vortex shedding is very important in engineering application to prevent the possible structural damages (Sudhakar & Vengadesan, 2012).

Previous works on the wake control of vortex shedding from a circular cylinder can be classified into two categories including active control and passive control. In the active control strategy, an input energy is required to be applied in the form of suction or blowing into the base region of the cylinder in order to control/reduce vortex shedding. However, in passive control strategy, an input energy is not required; instead, modifications of either the surface or the near-wake flow of the cylinder using some devices enables the reduction of vortex shedding (Yucel, Cetiner, & Unal, 2010). Among passive control approaches, the use of splitter plates has been one of the most successful methods which can lead to reduction and suppression of vortex street behind the cylinder (Kwon & Choi, 1996).

The splitter plates can be in the form of attached plates or detached plates. Early studies regarding the influence of splitter plates on cylinder wake was initiated by Roshko (1954). Roshko investigated the effect of splitter plate ratio ( $L/D$ , where  $L$  is the plate length and  $D$  is the cylinder diameter) on cylinder wake for a cylinder with an attached splitter plate. He reported that when the splitter plate was sufficiently long, e.g.  $L/D \geq 5$ , the vortex shedding was completely eliminated; hence, drag coefficient ( $C_D$ ) significantly reduced. The effect of splitter plate length was investigated by Gerrard (1966) at  $Re = 2 \times 10^4$ . He reported that increasing the length of the plate resulted in decreasing  $St$  within  $0 \leq L \leq D$ . However,  $St$  gradually increased by further increasing the plate length. Therefore, the minimum  $St$  was observed when the splitter plate ratio was approximately equal to one. He showed that the frequency of vortex shedding is inversely proportional to the vortex formation length ( $L_f$ ) immediately downstream of the bluff body. Similar experiments were conducted by Unal and Rockwell (1988) in the  $Re$  range of  $140 < Re < 1600$ . They divided the wake region into pre-vortex formation region and post-vortex formation region and observed a change in the pressure on the control plate when the plate was shifted from one region to another. Apelt, West, and Szewczyk (1973) and Apelt and West (1975) performed an experiment to study the effect of length of splitter plate for  $10^4 \leq Re \leq 5 \times 10^4$ . It was reported that the drag decreased as the length of the plate was increased up to  $L/D = 1$ . Then, it had an increasing trend within  $1 \leq L/D \leq 2$ , and after that, it decreased again. Apelt and West (1975) showed that adding the splitter plate led to a reduction in drag force and an enhancement in the base pressure. Moreover, similar trend was observed for the variation of  $C_D$  in comparison with the  $St$  variation at a higher  $Re (= 5 \times 10^4)$  in their experiments.

In addition to the above studies that considered attached splitters, there are studies that investigated the effect of detached splitter plates on cylinder wake. Roshko (1955) investigated the effects of adding detached splitter plate with splitter plate ratio of  $L/D = 1$ . He observed an increase in base pressure and a decrease in Strouhal number ( $St$ ) (a dimensionless number describing oscillating

flow mechanisms) when splitter plate was fixed downstream at a distance less than  $4D$ . Hwang, Yang, and Sun (2003) investigated the effects of a detached splitter plate on a circular cylinder and observed a considerable reduction of flow-induced forces on the cylinder. Akilli, Sahin, and Tumen (2005) extended the previous experimental studies to investigate the effects of detached splitter plate on the suppression of vortex shedding by varying the position of the plate. Ozono (2003) studied the effects of length and position of a detached splitter plate behind a cylinder at an asymmetric configuration. He observed that by increasing the gap between the cylinder base point and the leading edge of the downstream splitter plate, the values of  $St$  and  $C_D$  initially started decreasing. Serson, Meneghini, Carmo, Volpe, and Assi (2015) studied detached splitter plates and observed a strong dependence on  $Re$ , with the splitter plates being more beneficial at the higher values of Reynolds numbers.

More recently, Shukla, Govardhan, and Arakeri (2009) investigated the influence of attaching a hinged-rigid splitter plate to a cylinder on cylinder wake. Shukla stated that the communication between the shear layers downstream of the cylinder was not disrupted completely with using the hinged splitter plate. Furthermore, the splitter plate oscillated due to the pressure difference across the plate and the amplitude of oscillations reached to a maximum value of  $.45D$  at the free end. Similar investigations regarding the use of hinged rigid splitter plate attached to a cylinder were performed by Assi, Bearman, and Kitney (2009) and Gu, Wang, Qiao, and Huang (2012). There are also a few studies investigating the effect of a flexible splitter plate on flow quantities of the cylinder (Shukla, Govardhan, & Arakeri, 2013; Sudhakar & Vengadesan, 2012; Tian, Luo, Zhu, Liao, & Lu, 2011; De Nayer & Breuer, 2014). A number of recent studies have also investigated the use of dual-splitter plates in the wake control (Bao & Tao, 2013; Serson et al., 2015; Qiu, Sun, Wu, & Tamura, 2014; Barman & Bhattacharyya, 2015). Bao and Tao (2013) used short splitter plates of size  $L/D = .3$  for the wake control of vortex shedding. They also investigated the effect of length of the plates at a fixed position around the cylinder and observed that the length of the plates had crucial effects on drag reduction and wake suppression.

As discussed above, most of the previous works regarding the control and stabilisation of wake flow behind a cylinder only considered cylinders with one rigid splitter plate in a fixed angular position. The novelty of this paper is that it investigates the effects of having multiple rigid plates, attached to a cylinder on cylinder wake by comparing single-splitter, dual-splitters and tri-splitters cases. Moreover, the influence of the location of horizontal plates (attachment angle) on the cylinder wake is studied in the paper. This is followed by a more detailed study on the effect of the length of the middle plate in tri-splitters case on flow quantities. The same splitter plate ratio of  $L/D = 1$  which is greater than the length used in Bao and Tao (2013) study was initially considered for all the cases. The plates were located downstream of the cylinder and the variation of Strouhal number, drag coefficient and root-mean-square (r.m.s) value of the fluctuating

lift coefficient was investigated. The effect of the length of the middle plate in tri-splitters case was also investigated to support the initial findings obtained for this arrangement at  $L/D = 1$ . The commercial software, Comsol Multiphysics V.4.3a (COMSOL Inc., Stockholm, Sweden), was utilised to solve the problem using the finite element method.

The paper is organised as follows. The problem statement is given in Section 2. The numerical methodology used to solve the equations and validation of the numerical simulation, are presented in Section 3. The detailed results and the discussion are presented in Section 4 and final conclusions are given in Section 5.

## 2. Problem statement

In the present work, the problem of laminar flow past a circular cylinder is considered for three different cases: the cylinder with one, two and three rigid splitter plates attached to the rear surface of the cylinder as shown in Figure 1. In all these cases, the thickness of the plates ( $h$ ) was equal to  $.03D$ . The location of the horizontal plates behind the cylinder which was defined by attachment angle,  $\theta_p$ , (i.e. the angle between the wake centreline and a straight line crossing the centre of the cylinder and the attachment) was varied between  $\theta_p = 0^\circ$  and  $\theta_p = 90^\circ$ , leading to an asymmetric configuration for single-splitter case. However, in the cases of dual-splitters and tri-splitters, a symmetric configuration was assumed as can be seen in Figure 1.

The flow geometry and coordinate system as well as boundary conditions are shown in Figure 2. The computational domain was defined within  $-30D \leq x \leq 50D$  and  $-30D \leq y \leq 30D$ , where the centre of the cylinder was located at the origin ( $x = 0, y = 0$ ). The effect of the outlet boundary and the blockage effect were negligible in this problem as the size of the domain was large enough in both flow and cross-flow directions, respectively. The inlet velocity  $U$  was uniform, aligned with the  $x$ -direction and was chosen such that  $Re = \rho U_\infty D / \mu = 100$ . Pressure outlet boundary condition was applied on the far downstream outlet. Assuming the environment had the atmosphere conditions, a pressure value of zero was used on the outlet boundary. The open boundary conditions with no viscous stress were imposed to the lateral surfaces. A no-slip boundary condition specified as  $u_f = 0$  was applied on the cylinder wall and on the splitter plate, where  $u_f$  is the fluid velocity. Glycerine with dynamic viscosity of  $1.42 \frac{\text{kg}}{\text{m.s}}$  and density of  $1260 \frac{\text{kg}}{\text{m}^3}$  was used in the fluid domain.

The Reynolds number is defined as  $Re = \rho U_\infty D / \mu$ , where  $\rho$  and  $\mu$  are the density and dynamic viscosity of the fluid, respectively,  $U_\infty$  is the free-stream velocity and  $D$  is the diameter of the cylinder. Non-dimensional parameters, such as the drag coefficient ( $C_D$ ), the lift coefficient ( $C_L$ ), the Strouhal number ( $St$ ) and the pressure coefficient ( $C_p$ ) are defined by:

$$St = \frac{f_s D}{U_\infty} \quad (1)$$

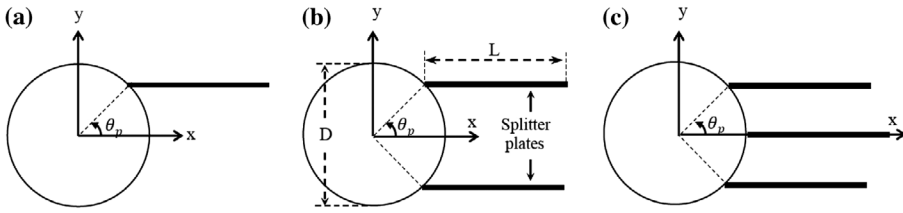


**Figure 1.** Schematic diagram of a cylinder with splitter plates. (a) Single-splitter, (b) dual-splitters, (c) tri-splitters.

where  $f_s$  is the vortex shedding frequency.

$$C_D = \frac{F_D}{.5\rho U_\infty^2 D} \quad (2)$$

$$C_L = \frac{F_L}{.5\rho U_\infty^2 D} \quad (3)$$

where  $\rho$  is the fluid density and  $F_D$  and  $F_L$  are the fluid forces (i.e. the pressure and viscosity forces) applied on the cylinder, in the streamwise and transverse directions, respectively.

$$C_p = \frac{P - P_\infty}{.5\rho U_\infty^2} \quad (4)$$

where  $p$  is the static pressure on the cylinder surface and  $P_\infty$  is the free-stream static pressure.

### 3. The numerical methodology and validation

#### 3.1. Governing equations and numerical formulation in Comsol multiphysics

The fluid flow is described by the mass continuity equation (Equation 4) and incompressible Navier-Stokes equation (Equation 5) (neglecting the volume forces):

$$\nabla \cdot u_f = 0 \quad (4)$$

$$\rho \left( \frac{\partial u_f}{\partial t} + u_f \cdot \nabla u_f \right) = \nabla \cdot [-pI + \mu(\nabla u_f + (\nabla u_f)^T)] \quad (5)$$

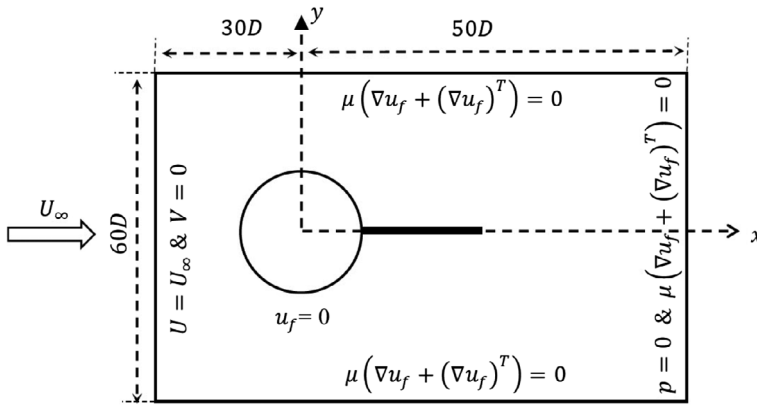


**Figure 2.** The computational domain and boundary conditions.

where  $\rho$  is the fluid density,  $p$  is the pressure,  $u_j$  is the velocity vector of the fluid and  $I$  is the unit diagonal matrix.

### 3.2. Finite element scheme

Comsol Multiphysics solves problems defined with Partial Differential Equations (PDEs) using Finite Element Method (FEM). In Comsol, Implicit Differential-Algebraic (IDA) solver is used to solve the system of equations which was attained from discretisation of the time-dependent PDE. IDA uses variable-order variable-step-size backward differentiation formulas (BDF) to discretise a PDE (Brown, Hindmarsh, & Petzold, 1994; Comsol, 2012; Hindmarsh et al., 2005).

The finite element equation of the discretised time-dependent PDE problem is given by:

$$0 = L(U, \dot{U}, \ddot{U}, t) - N_F(U, t)\Lambda \tag{6}$$

$$0 = M(U, t) \tag{7}$$

where  $U$  is the solution vector,  $L$  is the residual vector,  $M$  is the constraint residual,  $N_F$  is the constraint force Jacobian and  $\Lambda$  is a Lagrange multiplier.

A Newton solver is fitted into the IDA to solve the nonlinear system of equations which is generated due to the use of implicit time-stepping schemes. The attained equations which are linearised to be used in the Newton’s iteration are given by:

$$E\ddot{V} + D\dot{V} + KV = L - N_F\Lambda \tag{8}$$

$$NV = M \tag{9}$$

where  $V$  is the nodal displacement vector,  $K = \frac{-\partial L}{\partial U}$  is the stiffness matrix,  $D = \frac{-\partial L}{\partial \dot{U}}$  is the damping matrix,  $E = \frac{-\partial L}{\partial \ddot{U}}$  is the mass matrix and  $N$  is the constraint Jacobian matrix. A PARDISO (Parallel Direct Sparse Solver) solver is used by Newton solver to solve the resulting linear systems. PARDISO acts on general sparse linear systems of the form  $Ax = b$  and employs  $LU$  factorisation on the matrix  $A$  to find the solution  $x$  (Comsol, 2012; Schenk & Gärtner, 2004, 2006).

### 3.3. Validation of the finite element model

The simulation results were compared with experimental and numerical results from the literature for two benchmark cases at  $Re = 100$ : flow past a plain cylinder (the cylinder without any splitter plates), and flow past a plain cylinder with one splitter plate attached at  $\theta_p = 0^\circ$ . As shown in Table 1, the simulation results closely match other numerical (Hwang et al., 2003; Sudhakar & Vengadesan, 2012; Park, Kwon, & Choi, 1998; Kwon & Choi, 1996; Posdziech & Grundmann, 2007; Bao & Tao, 2013) and experimental (Williamson, 1989) results. The small differences between the present results and the numerical results from literature could be attributed to the different numerical approaches which have been implemented in the studies. Other possible reasons for the discrepancy of the numerical results in the different studies can include the blockage effect, the proximity of the cylinder to the inlet and the low cylinder distance from the outlet.

### 3.4. Grid independence test

Figure 3 shows the computational domain meshed using triangular and quadrilateral elements. Due to the high value of the velocity gradient near the cylinder wall and the plate wall, quadrilateral elements were used close to these regions. For the rest of the computational domain, triangular elements were used. The grid independence test was conducted on the flow past the cylinder with one splitter plate at  $\theta_p = 0^\circ$ . Four different mesh resolutions were used to examine the spatial convergence (Table 2).

**Table 1.** Comparison of characteristic quantities for flow past a circular cylinder with and without splitter plates.

Test cases	Flow quantities	Hwang et al. (2003)	Sudhakar and Vengadesan (2012)	Park et al. (1998)	Kwon and Choi (1996)	Williamson (1989)	Posdziech and Grundmann (2007)	Bao and Tao (2013)	Present
Plain cylinder,	$\overline{C_D}$	1.34	1.37	1.33	–	–	1.32	1.335	1.33
Re = 100	St	.167	.165	.164	–	.164	–	.164	.164
Single plate	$\overline{C_D}$	1.17	1.174	–	1.18	–	–	–	1.161
Re = 100, L/D=1	St	.137	.139	–	.137	–	–	–	.136

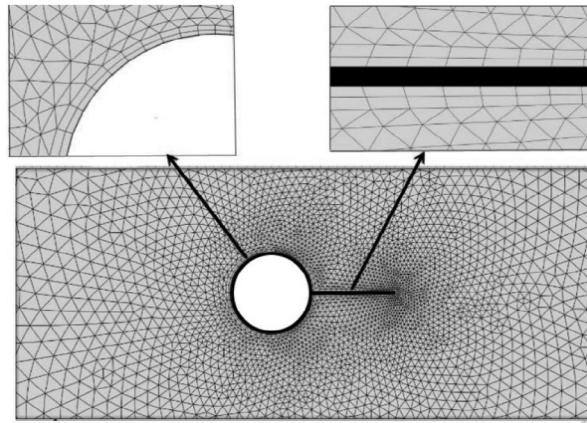


**Figure 3.** Mesh detail at the interface boundary between the plate wall and fluid domain.

**Table 2.** Grid independence test for the flow past a circular cylinder with one rigid splitter plate attached at  $\theta_p = 0^\circ$ .

Case	Grid elements	$\overline{C_D}$	St
(1)	1069	1.164	1.149
(2)	3450	1.162	1.144
(3)	11,976	1.161	1.144
(4)	29,495	1.161	1.144

Comparing the numerical results in Table 2, it can be seen that the mesh resolutions in case 1 and case 2 were appropriate to accurately evaluate the flow past over the cylinder. As the grid resolution was refined from case 2 to case 3, more accurate result was observed. However, further increase in mesh density (i.e. from case 3 to case 4) didn't cause significant change on the numerical measurements. Therefore, the mesh setting in case 3 which is computationally less expensive than case 4 was chosen for all subsequent simulations. A minimum mesh quality of .7323 in Comsol was used in this case for the fluid domain.

#### 4. Results and discussion

In this section, the effect of attaching one or more rigid splitter plates to the rear surface of the cylinder on Strouhal number (St), mean drag coefficient ( $\overline{C_D}$ ) and fluctuating lift coefficient ( $C_L$ ) is investigated. The results are presented against the location of the plates behind the cylinder which is defined by attachment angle ( $\theta_p$ ). In the case of cylinder with three attached splitters, the effect of the length of the plates is also investigated, focusing on the role of the middle plate in wake control.

#### 4.1. Vortex shedding frequency

The Strouhal number ( $St$ ) against attachment angle,  $\theta_p$ , for flow past a cylinder with one, two or three rigid splitters is presented in Figure 4. For comparison,  $St$  of the plain cylinder (the cylinder without any splitters) is also incorporated in the graph. The  $St$  was calculated from the period of the lift coefficient. It can be seen from Figure 4 that the cylinder with one rigid splitter plate had lower value of  $St$  than the plain cylinder. This can be attributed to the fact that the reaction between the shear layers downstream of the cylinder is delayed by the use of the splitter plate. It can also be seen that in the case of cylinder with single-splitter plate, by increasing  $\theta_p$  up to  $15^\circ$ , the  $St$  had a fixed value. However, by further increasing the attachment angle ( $15^\circ \leq \theta_p \leq 90^\circ$ ),  $St$  increased linearly. Therefore, a maximum shedding frequency reduction of 17% compared to the plain cylinder was achieved between  $\theta_p = 0^\circ$  and  $\theta_p = 15^\circ$  using the single-splitter.

Figure 5 illustrates the instantaneous streamlines for the flow past a cylinder with single-splitter (5a) and dual-splitters (5b). The increase in  $St$  occurred in single-splitter case within  $15^\circ \leq \theta_p \leq 90^\circ$  can be explained by looking at Figure 5(a). By increasing  $\theta_p$ , the upper vortex of the cylinder became narrower in the region close to the cylinder and grew in the region near the free end. On the other side, the lower vortex became larger and grew behind the cylinder under the plate (Figure 5(a)). This asymmetry results in separation of the upper vortex (the vortex behind the tip of the plate). Following that, the lower vortex can grow and shed, and the process repeats itself. It can also be seen from Figure 5(a) that by increasing  $\theta_p$  the asymmetry of vortex pairs with respect to the vortex positions, increased; thus, increasing  $St$ .

As can be seen from Figure 4, in the case of dual-splitters,  $St$  number remained constant between  $\theta_p = 0^\circ$  and  $\theta_p = 15^\circ$ , and the change in  $St$  number became

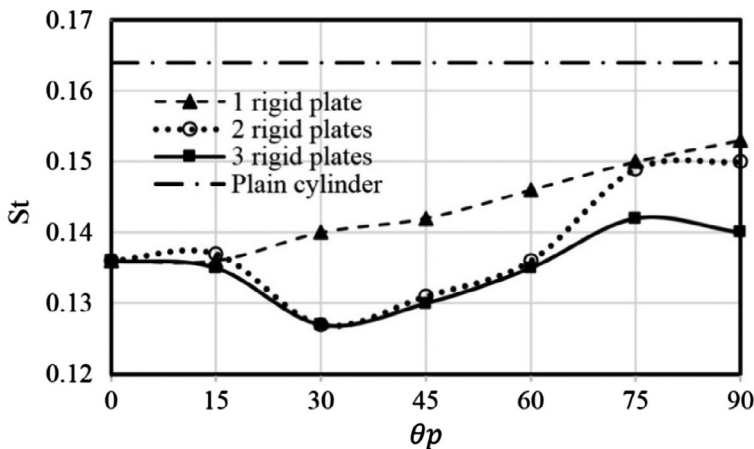


**Figure 4.** The variation of  $St$  number against the attachment angle in the three different splitter plate cases.

noticeable for  $\theta_p \geq 15^\circ$ . By increasing  $\theta_p$  in the range of  $15^\circ \leq \theta_p \leq 30^\circ$ , a reduction in St number occurred. This is because of the fact that increasing the distance between the two plates leads to a delay in the contact between the shear layers. Following that, the vortex formation length increases, resulting in decreasing the St number (Figure 5(b)). Then, by further increasing the attachment angle ( $30^\circ \leq \theta_p \leq 90^\circ$ ), the St number increased. This can be attributed to the reduction of vortex formation length as can be noticed from Figure 5(b). Similar trend can be seen for the tri-splitters up to  $\theta_p \approx 75^\circ$  (Figure 4). By further increasing  $\theta_p$ , the St number decreased due to the addition of the third plate (the middle plate). The middle plate prevented the growth of vortices in the region between the two plates; therefore, it led to a delay in contact between the vortices (Figure 6). Generally, the St number of the cylinder with one or more splitter plates in all attachment angles was always lower than that of the plain cylinder. Moreover, the St numbers associated with the cylinder with dual-splitters and tri-splitters are lower than that of the single-splitter, especially within  $20^\circ < \theta_p < 70^\circ$ . In the three different cases studied in this section, the lowest St was observed in cylinder with two/three splitter plates at  $\theta_p = 30^\circ$  in which the maximum shedding frequency reduction of

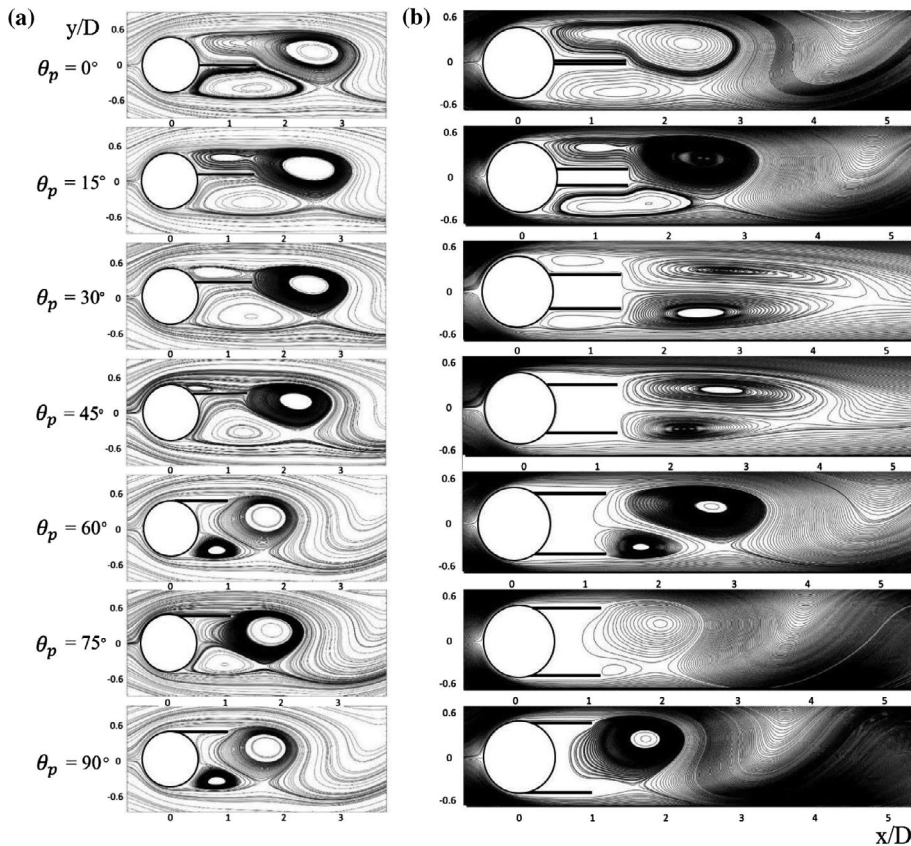


**Figure 5.** Instantaneous streamlines (a) cylinder with single-splitter and (b) cylinder with dual-splitters.

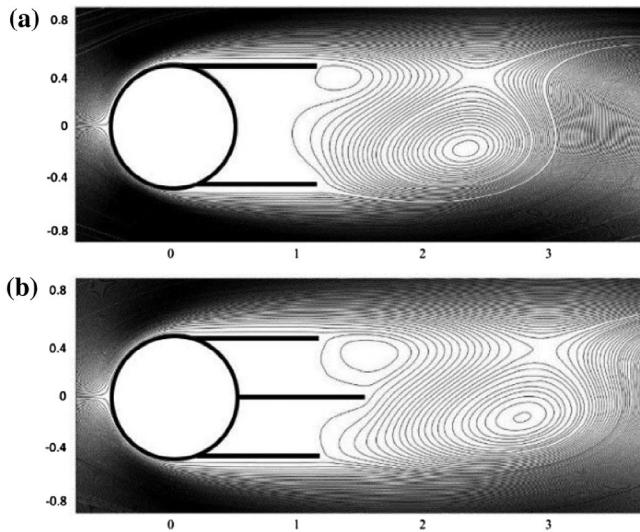


**Figure 6.** Instantaneous streamlines before lower vortex sheds at  $\theta_p = 75^\circ$  (a) cylinder with dual-splitters and (b) cylinder with tri-splitters.

22% in comparison with plain cylinder was achieved. Therefore, comparing with the single-splitter case, adding the second splitter plate had a significant effect in reducing the shedding frequency and improving the wake stabilisation.

#### 4.2. Mean drag force and fluctuating lift force

Figure 7 shows the mean drag coefficient,  $\overline{C_D}$ , which was numerically calculated for the different considered cases.  $\overline{C_D}$  in Figure 7(a) was computed from integration of pressure and viscous stresses over the cylinder surface only, while  $\overline{C_{Df}}$  in Figure 7(b) was computed from integration over both the cylinder and plates walls. Moreover, the reference results of drag coefficient for the plain cylinder were incorporated into the figures for comparison. It can be seen from Figure 7(a) and (b) that a significant reduction in drag coefficient was achieved by the use of splitter plates in all the three cases compared to the plain cylinder. It can also be seen that dual-splitters and tri-splitters cases had lower values of drag coefficient than the single-splitter case.

It can also be seen from Figure 7(a) that in the case of the cylinder with one splitter plate, by increasing  $\theta_p$ ,  $\overline{C_D}$  remained almost constant within  $0^\circ \leq \theta_p \leq 15^\circ$ . Then,  $\overline{C_D}$  decreased until it reached a minimum value at  $\theta_p = 45^\circ$ . In this position the maximum drag reduction of 15% was attained compared to the plain cylinder. After that, by further increasing  $\theta_p$  up to  $90^\circ$ ,  $\overline{C_D}$  increased up to almost its initial value at  $0^\circ$ . In the dual-splitters case, by increasing  $\theta_p$  up to  $45^\circ$ , a similar trend as the single-splitter plate case can be observed between  $\theta_p = 0^\circ$  and  $\theta_p = 45^\circ$ . However, the value of  $\overline{C_D}$  of the cylinder with dual-splitters was considerably smaller than the one with a single-splitter plate, especially within  $45^\circ \leq \theta_p \leq 90^\circ$ .

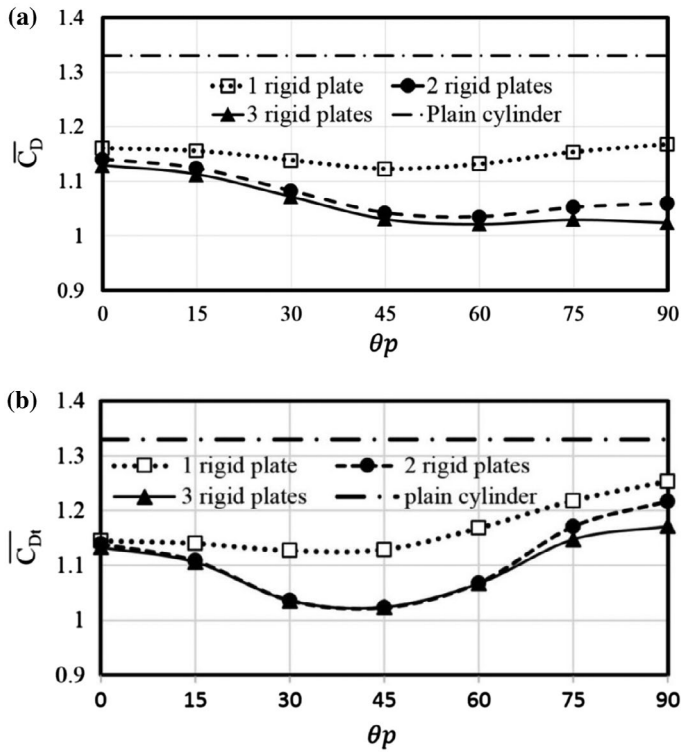


**Figure 7.** Mean drag coefficient, (a)  $\overline{C_D}$  and (b)  $\overline{C_{Dt}}$ , against the attachment angle of the splitter plates,  $\theta_p$ .

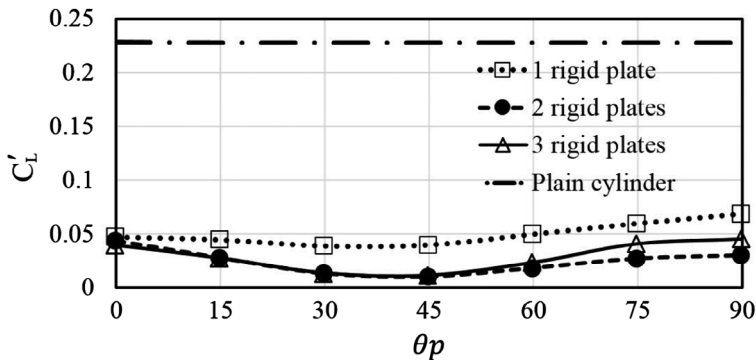
In this case, a maximum drag reduction of 23% compared to the plain cylinder case was observed at  $\theta_p = 45^\circ$ . Our numerical result for drag coefficient at  $\theta_p = 40^\circ$  ( $\overline{C_D} = 1.210$ ) matches closely with that obtained by Bao and Tao (2013) ( $\overline{C_D} = 1.215$ ) for the same dual-splitter configuration. In the case of cylinder with tri-splitters as can be seen in Figure 7(a), the  $\overline{C_D}$  was very close to that of the dual-splitters, showing that adding the third plate (middle plate in tri-splitter plate case) didn't have considerable effect on the drag coefficient.

It can be seen from Figure 7(b) that a similar trend as  $\overline{C_D}$  was observed for  $\overline{C_{Dt}}$  in all three cases between  $\theta_p = 0^\circ$  and  $\theta_p = 45^\circ$ . However, by further increasing  $\theta_p$ ,  $\overline{C_{Dt}}$  had a higher rate of growth compared to  $\overline{C_D}$  between  $\theta_p = 60^\circ$  and  $\theta_p = 90^\circ$  in all the simulated cases. This observation can be attributed to viscosity effect of the plates which has an increasing trend for  $\theta_p > 60^\circ$ . As can be seen from Figure 5(a) and (b), in low attachment angles ( $0^\circ \leq \theta_p \leq 45^\circ$ ), a vortex is formed between the plate and the main stream, reducing the effect of viscous drag due to the lack of contact between the surfaces of the plates and the main stream. In this position, the viscous component of the drag coefficient is expected to be significantly smaller than the pressure component. Hence, the plots of  $\overline{C_D}$  and  $\overline{C_{Dt}}$  (Figure 7(a) and (b)) share the same profile in this region. However, by increasing the attachment angle, especially when  $\theta_p \geq 60^\circ$ , the viscous component of the drag coefficient becomes

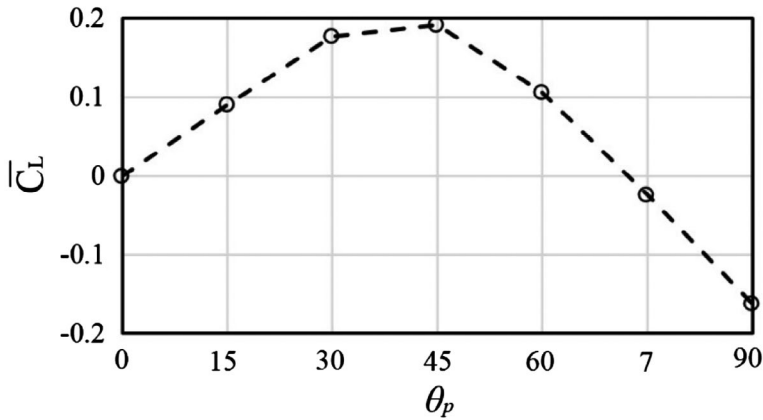
more effective due to the contact between the plates surfaces and the main stream. Therefore, the plots of  $\overline{C_D}$  and  $\overline{C_{Dt}}$  have different trends at  $\theta_p \geq 60^\circ$ . Consequently, dual-splitter are more influenced by this effect than a single-splitter. However, attaching third plate in the middle (tri-splitter case), doesn't cause significant change in viscous drag, due to the lack of effective contact between the surfaces of the middle plate and the main flow.

Figure 8 shows the root-mean-square (r.m.s.) value of the fluctuating lift coefficient ( $C'_L$ ) which represents the influence of the splitter plates on the wake oscillation against attachment angle,  $\theta_p$ . The corresponding value of  $C'_L$  for plain cylinder is incorporated to the figure for comparison. As can be seen from Figure 8, by changing the position of the plates,  $C'_L$  has a similar trend as drag coefficient studied earlier in this section. Hence, the use of splitter plates attached to a circular cylinder can lead to reduction in wake oscillation. However, this reduction in dual-splitter and tri-splitter cases (which share similar profile) is more than the corresponding value of the cylinder with single-splitter.  $C'_L$  had a decreasing trend by increasing the attachment angle within  $0^\circ \leq \theta_p \leq 45^\circ$  and reached to its minimum at  $\theta_p = 45^\circ$  (in all three cases). At this position, a maximum reduction of 95% in  $C'_L$  was observed in dual-splitter and tri-splitter compared to  $C'_L$  of the plain cylinder.

Also, it is interesting to see how much the average lift coefficient ( $\overline{C_L}$ ) is affected when using only one splitter at various positions. As can be seen from Figure 9, by increasing the attachment angle,  $\overline{C_L}$  increased until it reached to its maximum value at  $\theta_p = 45^\circ$ . By further increasing the attachment angle,  $\overline{C_L}$  reduced and reached to zero at  $\theta_p \approx 70^\circ$ , and continued decreasing to negative values after that.



**Figure 8.** The r.m.s. value of the lift coefficient ( $C'_L$ ), against the attachment angle of the splitter plates,  $\theta_p$ .



**Figure 9.** The average lift coefficient ( $\overline{C_L}$ ), against the attachment angle of the splitter plate,  $\theta_p$ , in cylinder with single-splitter.

### 4.3. Pressure distribution on the cylinder surface

The change in the drag coefficient and average lift coefficient investigated earlier in this paper are directly related to the pressure distribution. Figure 10 shows the mean pressure coefficient,  $\overline{C_p}$ , against the angular position around the cylinder ( $\theta$ ) with one or two splitter plates attached at various positions ( $\theta_p$ ). For the single-splitter case because of the asymmetric configuration, the figure was plotted in the range of  $-120^\circ \leq \theta \leq 120^\circ$  and for the dual-splitters, due to the symmetric configuration, the figure was plotted in the range of  $0^\circ \leq \theta \leq 120^\circ$ . Outside  $-120^\circ \leq \theta \leq 120^\circ$ , curves shared the same profile; therefore, they are not plotted in the figures. It can be seen that in the single-splitter case (Figure 10(a)) as well as the dual-splitters (Figure 10(b)), the results are set into two regions of the curves. In the region between the wake centreline ( $\theta = 0$ ) and the plate ( $\theta = \theta_p$ ), the pressure distribution was significantly influenced by the value of  $\theta$ , whereas in the other region ( $\theta > \theta_p$ ), the mean pressure coefficient had a similar trend against  $\theta$ . Therefore, we focused on the feature displayed within the region between the wake centreline and the plate ( $0 \leq \theta \leq \theta_p$ ). In this region, the values of  $-\overline{C_p}$  for the cylinder with single-splitter (Figure 10(a)) and cylinder with dual-splitters (Figure 10(b)) for all plate positions (attachment angles) were smaller than the associated value of the plain cylinder. Because of that, the values of  $\overline{C_D}$  in single-splitter and dual-splitters cases for all attachment angles were smaller than  $\overline{C_D}$  of the plain cylinder, as was seen in Figure 7(a).

It can be seen in Figure 10(b) that in the case of cylinder with dual-splitters,  $\overline{C_p}$  had a fixed value in the region between the wake centreline and the plate ( $0 < \theta < \theta_p$ ). Similarly in tri-splitters,  $\overline{C_p}$  will have a fixed value in the region between the plates ( $0 < \theta < \theta_p$ ). Therefore, the variation of  $\overline{C_D}$  against attachment angle in the tri-splitters case can be justified by the behaviour of the mean base pressure coefficient,  $\overline{C_{pb}} \left( = \frac{P_b - P_\infty}{.5\rho U_\infty^2} \right)$  where  $P_b$  is the static pressure on the

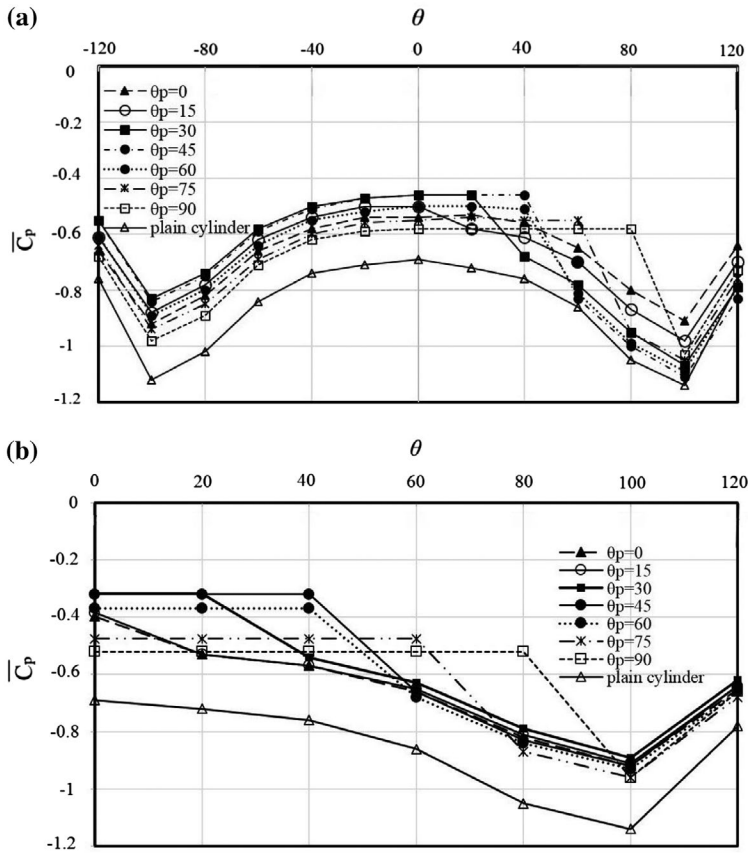


**Figure 10.** The mean pressure coefficient distribution,  $\overline{C_p}$ , against the angular position around the cylinder,  $\theta$ , in various attachment angle ( $\theta_p$ ) of splitter plates at downstream for (a) cylinder with single-splitter and (b) cylinder with dual-splitters.

cylinder surface at  $\theta = 0^\circ$ . The variation of mean base pressure coefficient,  $\overline{C_{pb}}$ , against the attachment angle for the tri-splitters case is illustrated in Figure 11. Moreover, the value of  $\overline{C_{pb}}$  in the case of cylinder with dual-splitters, as well as the plain cylinder is incorporated into the figure for comparison. It can be seen that the plots of the dual-splitters and tri-splitters share almost the same profile within  $0^\circ \leq \theta_p \leq 75^\circ$ . Therefore, the value of  $\overline{C_D}$  in tri-splitters is close to that in dual-splitters in this range (Figure 7(a)). However, by further increasing  $\theta_p$ ,  $-\overline{C_{pb}}$  in tri-splitters becomes smaller than that in dual-splitters; thus, resulting in a lower value of  $\overline{C_D}$  compared to that in dual-splitters.

#### 4.4. The effect of the length of middle plate in tri-splitters

The effect of the plate length on flow quantities for single-splitter was investigated in a number of previous studies (Apelt & West, 1975; Apelt et al., 1973; Bearman, 1965; Kwon & Choi, 1996). Findings showed that the cylinder wake was highly

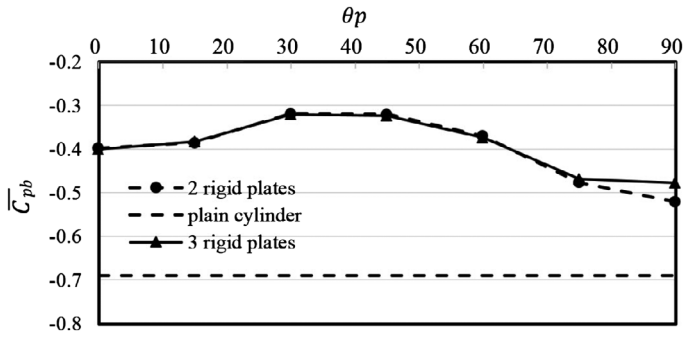


**Figure 11.** The mean base pressure coefficient,  $\overline{C_{pb}}$ , against attachment angle,  $\theta_p$ , in tri-splitters case compared with the plain cylinder and cylinder with two splitter plates.

influenced by the length of the splitter plate. In Section 4.2 of the paper, it was observed that adding the third splitter plate of the same length, didn't have significant effect on the drag coefficient when compared with dual-splitters. In this section, in order to clarify the effect of adding the third plate on flow quantities, the length of the middle plate ( $L_{mid}$ ) in tri-splitters was changed within  $0 \leq L_{mid}/D \leq 4$  at a fixed attachment angle of  $45^\circ$  which is associated with the position of two lateral splitters where the minimum value of drag was observed. Two different scenarios were considered based on the length of the lateral plates ( $L_{lat}$ ); tri-splitters with two long lateral plates of size  $L_{lat}/D = 1$ , and tri-splitters with two short lateral plates of size  $L_{lat}/D = .3$ . Figure 12 shows the change in drag coefficient by varying the length of the middle plate ( $L_{mid}$ ). It can be seen that with long lateral plates, the change in drag coefficient against the length of the middle plate was not noticeable. This is due to the fact that in this situation, the middle plate is located in a zone with no wake. However, when short lateral plates were utilised ( $L_{lat}/D = .3$ ), it can be seen that increasing the length of the middle plate led to reduction of drag coefficient. In this case a maximum reduction of 7% was achieved when size of the middle plate was  $L_{mid}/D = 2$ . However, further increase in the length of the middle didn't have noticeable effect on the value of drag coefficient.

Figure 13 shows r.m.s. value of the lift coefficient ( $C'_L$ ) against the dimensionless length of the middle plate ( $L_{mid}/D$ ). It can be seen that when short lateral plates ( $L_{lat}/D = .3$ ) were used, by increasing the length of the middle plate up to  $L_{mid}/D = 2.1$ ,  $C'_L$  has significantly decreased. In this case, increasing the length of the middle plate beyond  $L_{mid}/D = 2.1$  has resulted in complete prevention of the wake oscillations. However,  $C'_L$  of tri-splitters with long lateral plates is considerably lower than the corresponding value of tri-splitters with short lateral plates. In this case, increasing the length of the middle plate beyond  $L_{mid}/D = 1.5$  has resulted in complete prevention of the wake oscillations.

The variation of mean base pressure coefficient,  $\overline{C_{pb}}$ , against the dimensionless length of the middle plate ( $L_{mid}/D$ ) in tri-splitters is illustrated in Figure 14. It can be

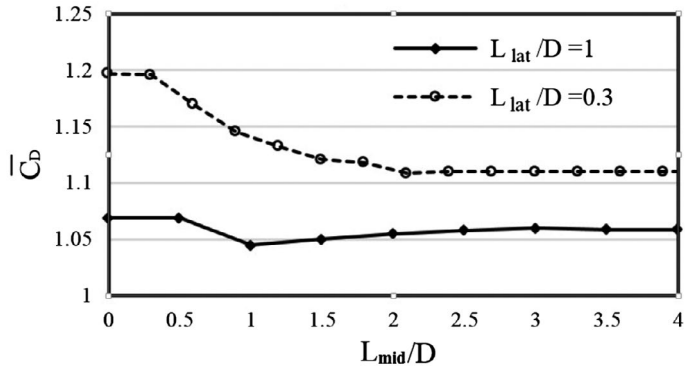


Figure 12. Mean drag coefficient,  $\overline{C_D}$ , against the dimensionless length of the middle plate ( $L_{mid}/D$ ) in two different cases:  $L_{lat}/D = .3$  and  $L_{lat}/D = 1$ .

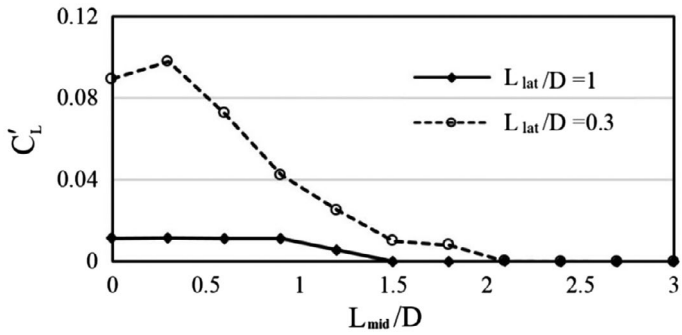


Figure 13. r.m.s. value of the lift coefficient ( $C_l'$ ), against the dimensionless length of the middle plate ( $L_{mid}/D$ ) in two different cases:  $L_{lat}/D = .3$  and  $L_{lat}/D = 1$ .

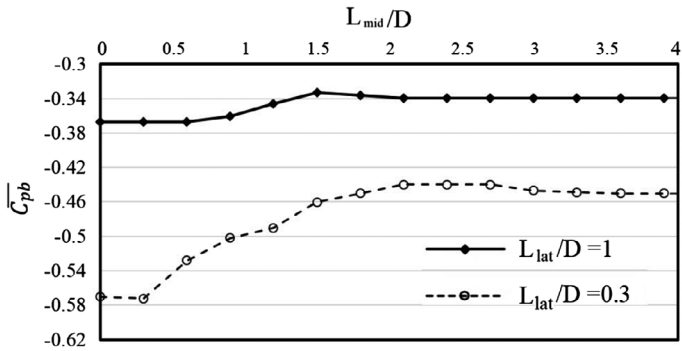


Figure 14. The mean base pressure coefficient,  $\overline{C_{pb}}$ , against the dimensionless length of the middle plate ( $L_{mid}/D$ ) in two different cases:  $L_{lat}/D = .3$  and  $L_{lat}/D = 1$ .

seen that in the case of tri-splitters with short lateral plates ( $L_{\text{lat}}/D = .3$ ), by increasing the length of the middle plate,  $-\overline{C_{pb}}$  has decreased and resulted in a decrease in  $\overline{C_D}$  (as was seen in Figure 12). However, in the case of tri-splitters with long lateral plates ( $L_{\text{lat}}/D = 1$ ), there was no considerable change in  $-\overline{C_{pb}}$  by increasing  $L_{\text{mid}}$ , similar to what was observed for the corresponding  $\overline{C_D}$  in Figure 12.

## 5. Summary and conclusions

A numerical investigation of the flow over a cylinder with up to three attached rigid splitter plates was performed in this work and the time-averaged characteristics were measured. The length of the plates was initially chosen to be equal to the cylinder diameter and the position of the plates was described by their attachment angle which was varied between  $0^\circ$  and  $90^\circ$ . The main findings are as follows:

- Increasing the number of attached plates, from one to two, had a crucial effect on reduction of drag coefficient, Strouhal number and r.m.s. value of the lift coefficient. However, further increase to three plates, didn't have a significant effect on these quantities.
- The minimum drag coefficient was observed in the attachment angle of  $45^\circ$ . In this position, 15% reduction of drag coefficient was achieved for the cylinder with one attached splitter plate, and 23% reduction was achieved for the cylinders with two and three attached splitter plates, compared to the drag coefficient of a plain cylinder.
- In dual-splitters and tri-splitters cases, a maximum of 95% reduction in r.m.s. value of the lift coefficient compared to the corresponding value of the plain cylinder was achieved at  $\theta_p = 45^\circ$ .
- In single-splitter plate case, the average value of lift coefficient was highly dependent on the position of the attached plate and the maximum value was observed at  $\theta_p \approx 45^\circ$ .
- In the single-splitter case, the minimum St was observed in the attachment angle of approximately  $0^\circ$  which resulted in 17% reduction of St compared to the plain cylinder. In the dual-splitters and tri-splitters cases, the minimum St was observed in the attachment angle of  $30^\circ$  in which 22% reduction of St was achieved compared to the plain cylinder.
- Although in tri-splitters case initially investigated ( $L/D = 1$ ), the effect of the middle plate on flow quantities was not considerable, it was observed that when lateral plates are short, for instance  $L_{\text{lat}}/D = .3$ , the effect of the length of the middle plate on controlling the flow past the cylinder becomes noticeable.

To sum up, the results of this study suggest that drag on cylinder, vortex shedding frequency and fluctuations of lift coefficient can be effectively reduced by attaching one or more splitter plates placed in appropriate position. Assuming splitters are of the same length, the use of two parallel splitters symmetrically attached to the cylinder is recommended. The current investigation sheds light on the future developments of efficient drag controlling methods for a cylinder immersed in a free stream.

## Disclosure statement

No potential conflict of interest was reported by the authors.

## ORCID

Rezvan Abdi  <http://orcid.org/0000-0002-1015-050X>

Meisam Abdi  <http://orcid.org/0000-0003-2320-7509>

## References

- Akilli, H., Sahin, B., & Tumen, N. F. (2005). Suppression of vortex shedding of circular cylinder in shallow water by a splitter plate. *Flow Measurement and Instrumentation*, 16, 211–219.
- Apelt, C. J., & West, G. S. (1975). The effects of wake splitter plates on bluff-body flow in the range  $10^4 < R < 5 \times 10^4$ . Part 2. *Journal of Fluid Mechanics*, 71, 145–160.
- Apelt, C. J., West, G. S., & Szewczyk, A. A. (1973). The effects of wake splitter plates on the flow past a circular cylinder in the range  $10^4 < R < 5 \times 10^4$ . *Journal of Fluid Mechanics*, 61, 187–198.
- Assi, G. R., Bearman, P. W., & Kitney, N. (2009). Low drag solutions for suppressing vortex-induced vibration of circular cylinders. *Journal of Fluids and Structures*, 25, 666–675.
- Bao, Y., & Tao, J. (2013). The passive control of wake flow behind a circular cylinder by parallel dual plates. *Journal of Fluids and Structures*, 37, 201–219.
- Barman, B., & Bhattacharyya, S. (2015). Control of vortex shedding and drag reduction through dual splitter plates attached to a square cylinder. *Journal of Marine Science and Application*, 14, 138–145.
- Bearman, P. W. (1965). Investigation of the flow behind a two-dimensional model with a blunt trailing edge and fitted with splitter plates. *Journal of Fluid Mechanics*, 21, 241–255.
- Brown, P. N., Hindmarsh, A. C., & Petzold, L. R. (1994). Using Krylov methods in the solution of large-scale differential-algebraic systems. *SIAM Journal on Scientific Computing*, 15, 1467–1488.
- COMSOL Multiphysics, COMSOL Multiphysics User Guide (Version 4.3 a), 2012. COMSOL, AB.
- De Nayer, G., & Breuer, M. (2014). Numerical FSI investigation based on LES: Flow past a cylinder with a flexible splitter plate involving large deformations (FSI-PfS-2a). *International Journal of Heat and Fluid Flow*, 50, 300–315.
- Gerrard, J. H. (1966). The mechanics of the formation region of vortices behind bluff bodies. *Journal of Fluid Mechanics*, 25, 401–413.
- Gu, F., Wang, J. S., Qiao, X. Q., & Huang, Z. (2012). Pressure distribution, fluctuating forces and vortex shedding behavior of circular cylinder with rotatable splitter plates. *Journal of Fluids and Structures*, 28, 263–278.
- Hindmarsh, A. C., Brown, P. N., Grant, K. E., Lee, S. L., Serban, R., Shumaker, D. E., & Woodward, C. S. (2005). SUNDIALS: Suite of nonlinear and differential/algebraic equation solvers. *ACM Transactions on Mathematical Software*, 31, 363–396.
- Hwang, J. Y., Yang, K. S., & Sun, S. H. (2003). Reduction of flow-induced forces on a circular cylinder using a detached splitter plate. *Physics of Fluids*, 15, 2433–2436 (1994-present).
- Kwon, K., & Choi, H. (1996). Control of laminar vortex shedding behind a circular cylinder using splitter plates. *Physics of Fluids*, 8, 479–486 (1994-present).
- Ozono, S. (2003). Vortex suppression of the cylinder wake by deflectors. *Journal of Wind Engineering and Industrial Aerodynamics*, 91, 91–99.
- Park, J., Kwon, K., & Choi, H. (1998). Numerical solutions of flow past a circular cylinder at Reynolds numbers up to 160. *KSME International Journal*, 12, 1200–1205.

- Posdziech, O., & Grundmann, R. (2007). A systematic approach to the numerical calculation of fundamental quantities of the two-dimensional flow over a circular cylinder. *Journal of Fluids and Structures*, 23, 479–499.
- Qiu, Y., Sun, Y., Wu, Y., & Tamura, Y. (2014). Effects of splitter plates and Reynolds number on the aerodynamic loads acting on a circular cylinder. *Journal of Wind Engineering and Industrial Aerodynamics*, 127, 40–50.
- Roshko, A. (1954). *On the drag and shedding frequency of two-dimensional bluff bodies* (No. TN3169). Washington, DC: National Aeronautics and Space Administration.
- Roshko, A. (1955). On the wake and drag of bluff bodies. *Journal of the Aeronautical Sciences (Institute of the Aeronautical Sciences)*, 22, 124–132.
- Schenk, O., & Gärtner, K. (2004). Solving unsymmetric sparse systems of linear equations with PARDISO. *Future Generation Computer Systems*, 20, 475–487.
- Schenk, O., & Gärtner, K. (2006). On fast factorization pivoting methods for sparse symmetric indefinite systems. *Electronic Transactions on Numerical Analysis*, 23, 158–179.
- Serson, D., Meneghini, J. R., Carmo, B. S., Volpe, E. V., & Assi, G. R. S. (2015). Numerical study of the flow around a circular cylinder with dual parallel splitter plates. In V. Theofilis & J. Soria (Eds.), *Instability and Control of Massively Separated Flows* (pp. 169–174). Cham: Springer International Publishing.
- Shukla, S., Govardhan, R. N., & Arakeri, J. H. (2009). Flow over a cylinder with a hinged-splitter plate. *Journal of Fluids and Structures*, 25, 713–720.
- Shukla, S., Govardhan, R. N., & Arakeri, J. H. (2013). Dynamics of a flexible splitter plate in the wake of a circular cylinder. *Journal of Fluids and Structures*, 41, 127–134.
- Sudhakar, Y., & Vengadesan, S. (2012). Vortex shedding characteristics of a circular cylinder with an oscillating wake splitter plate. *Computers & Fluids*, 53, 40–52.
- Tian, F. B., Luo, H., Zhu, L., Liao, J. C., & Lu, X. Y. (2011). An efficient immersed boundary-lattice Boltzmann method for the hydrodynamic interaction of elastic filaments. *Journal of Computational Physics*, 230, 7266–7283.
- Unal, M. F., & Rockwell, D. (1988). On vortex formation from a cylinder. Part 1. The initial instability. *Journal of Fluid Mechanics*, 190, 491–512.
- Williamson, C. H. K. (1989). Oblique and parallel modes of vortex shedding in the wake of a circular cylinder at low Reynolds numbers. *Journal of Fluid Mechanics*, 206, 579–627.
- Yucel, S. B., Cetiner, O., & Unal, M. F. (2010). Interaction of circular cylinder wake with a short asymmetrically located downstream plate. *Experiments in Fluids*, 49, 241–255.